Drug Design, Development and Therapy Dovepress

Open Access Full Text Article ORIGINAL RESEARCH

Protopine Exerts Neuroprotective Effects on Neonatal Hypoxic-Ischemic Brain Damage in Rats via Activation of the AMPK/PGC1α Pathway

Liying Lu[1,2], Mengdan Pang[1,2], Tingting Chen[1,2], Yingying Hu[1,2], Likai Chen[3], Xiaoyue Tao[1,2], Shangqin Chen[1,2], Jianghu Zhu[1,2], Mingchu Fang[1,2], XiaoLing Guo[1,4], Zhenlang Lin[1,2,4]

[1]Department of Pediatrics, The Second School of Medicine, The Second Affiliated Hospital and Yuying Children's Hospital of Wenzhou Medical University, Wenzhou, Zhejiang, People's Republic of China; [2]Key Laboratory of Perinatal Medicine of Wenzhou, the Second Affiliated Hospital and Yuying Children's Hospital of Wenzhou Medical University, Wenzhou, Zhejiang, People's Republic of China; [3]Elson S. Floyd College of Medicine at Washington State University, Spokane, WA, USA; [4]Basic Medical Research Center, the Second Affiliated Hospital and Yuying Children's Hospital of Wenzhou Medical University, Wenzhou, Zhejiang, People's Republic of China

Correspondence: XiaoLing Guo; Zhenlang Lin, The Second Affiliated Hospital and Yuying Children's Hospital of Wenzhou Medical University, 109 Xueyuan West Road, Wenzhou, Zhejiang, 325027, People's Republic of China, Tel +00-86-138-0668-9800, Fax +86-0577-88002198, Email guoxling@hotmail.com; linzhenlang@hotmail.com

Introduction: Neonatal hypoxic-ischemic encephalopathy (HIE), caused by perinatal asphyxia, is characterized by high morbidity and mortality, but there are still no effective therapeutic drugs. Mitochondrial biogenesis and apoptosis play key roles in the pathogenesis of HIE. Protopine (Pro), an isoquinoline alkaloid, has anti-apoptotic and neuro-protective effects. However, the protective roles of Pro on neonatal hypoxic-ischemic brain injury remain unclear.

Methods: In this study, we established a $CoCl_2$-induced PC12 cell model in vitro and a neonatal rat hypoxic-ischemic (HI) brain damage model in vivo to explore the neuro-protective effects of Pro and try to elucidate the potential mechanisms.

Results: Our results showed that Pro significantly reduced cerebral infarct volume, alleviated brain edema, inhibited glia activation, improved mitochondrial biogenesis, relieved neuron cell loss, decreased cell apoptosis and reactive oxygen species (ROS) after HI damage. In addition, Pro intervention upregulated the levels of p-AMPK/AMPK and PGC1α as well as the downstream mitochondrial biogenesis related factors, such as nuclear respiratory factor 1 (NRF1) and mitochondrial transcription factor A (TFAM), but the AMPK inhibitor compound c (CC) could significantly reverse these effects of Pro.

Discussion: Pro may exert neuroprotective effects on neonatal hypoxic-ischemic brain damage via activation of the AMPK/PGC1α pathway, suggesting that Pro may be a promising therapeutic candidate for HIE, and our study firstly demonstrate the neuro-protective roles of Pro in HIE models.

Keywords: neonatal hypoxic-ischemic brain damage, protopine, reactive oxygen species, apoptosis, mitochondrial biogenesis

Introduction

Neonatal hypoxic-ischemic encephalopathy (HIE) is an important cause of neonatal death or nervous system dysfunction during pregnancy and delivery.[1] More than half of HIE neonates die in the neonatal period, and those who survive are at a high risk of neurological sequelae such as, cerebral palsy and intellectual disability.[2] Hypothermia is the only clinically approved treatment method, but the time window of hypothermia is very narrow, only 6 h.[3] In addition, a variety of emerging treatment methods are currently being explored, such as stem cell therapy, growth factor therapy, anti-inflammatory drugs, antioxidant therapy, etc.[4,5] However, these treatments may carry risks such as unknown safety or poor efficacy in clinical trials. Therefore, it is imperative to explore more effective drugs to improve the prognosis of neonatal HIE.

The pathomechanism of neonatal HIE is a complex evolutionary process, including inflammation, oxidative stress, excitotoxicity, and mitochondrial damage, leading to progressive neuronal cell death.[4,6] When the brain undergoes

Received: 30 June 2024
Accepted: 26 October 2024
Published: 5 November 2024

ischemia and hypoxia, a series of destructive changes, such as insufficient energy supply, excessive reactive oxygen species (ROS) generation, and neuronal apoptosis, can occur, which are the basis of neurological dysfunction.[7] Mitochondria are not only the energy factories of ATP required for neuronal excitability and survival, but are also involved in ROS and apoptosis, which are important inducements for neurodegenerative diseases.[8] The increasing studies have also proven that excessive ROS from impaired mitochondrial biogenesis is closely related to neuronal death.[9,10] More studies have explored the correlation between HIE and mitochondrial biogenesis. Swimming has been found to stabilize mitochondrial cristae and improve motor, memory, and learning-related activities.[11] Yin et al first demonstrated a rapid increase in mitochondrial biogenesis after 24 h of neonatal rat HIE and suggested that increasing mitochondrial mass will significantly improve the overall oxidative function and energy status of the brain after HIE.[12] Therefore, improving mitochondrial biogenesis may become a key therapeutic target.

Adenosine 5'monophosphate-activated protein kinase (AMPK) is a cellular energy sensor that restores ATP concentration by reducing anabolism and energy consumption.[13] Under low-oxygen environments, hypoxia impairs the ability of mitochondria to efficiently conduct oxidative phosphorylation, thereby reducing ATP synthesis. This situation of energy deficiency raises the AMP/ATP ratio, which activates AMPK.[14] Activation of AMPK at Thr172 was found to up-regulate peroxisome proliferator-activated receptor γ (PPARγ) coactivator 1α (PGC1α).[8] PGC1α is abundant in the brain.[15] More importantly, PGC-1α enters the nucleus and combines with nuclear respiratory factor 1 (NRF1), up-regulating the expression of mitochondrial DNA-binding protein mitochondrial transcription factor A (TFAM), promoting mitochondrial synthesis, regulating mitochondrial homeostasis, and reducing the generation of ROS.[16–18] Under low-oxygen conditions, AMPK/PGC1α regulation of mitochondrial biogenesis improves neuronal stress resistance, reduces cell hypoxia damage, maintains metabolic homeostasis, and ensures survival and normal functions.[8] Therefore, identifying exogenous compounds that can increase mitochondrial biogenesis is crucial for treating neonatal HIE.

Protopine (Pro) is an isoquinoline alkaloid extracted from a variety of plants.[19] It is involved in numerous biological processes, including antioxidation, anti-colon cancer, anti-inflammatory, antifungal, and anti-hepatotoxic properties.[19–25] It has also been shown to cross the blood-brain barrier and has anti-depressant effects in the neurological system.[26,27] A study using a cerebral ischemia model of male Sprague-Dawley (SD) rats showed that Pro could significantly reduce cerebral infarction and increase the activity of superoxide dismutase (SOD) in serum.[28] Furthermore, Pro could partially alleviate H_2O_2-induced oxidative stress and apoptosis in PC12 cells through Ca (2+) antagonism and anti-oxidant mechanisms.[22] Although Pro is derived from natural plants and has a good safety profile, high concentrations (>40 μM) of Pro can impair cardiac function and have toxic effects on normal cells.[29,30]

So far, there is no report to explore the neuro-protective roles of Pro on neonatal HI brain damage. $CoCl_2$ that can trigger ROS production and increase the expression level of hypoxia-inducible factor 1 (HIF-1), is widely used to induce hypoxic-ischemic states.[31] Neonatal rat hypoxic-ischemic brain damage (HIBD) models were established according to the modified Vannucci model.[32] This model mimics ischemia and hypoxia to replicate a variety of cellular and molecular characteristics of HIE, including neuronal necrosis, cerebral hemorrhage, neuronal apoptosis, and neuronal karyopyknosis and other brain histopathological changes. Considering the roles of mitochondrial biogenesis in oxidative stress and apoptosis, we hypothesized that AMPK/PGC1α may be involved in the pathogenesis of neonatal HIE by promoting mitochondrial biogenesis. The objective of this study is to investigate Pro neuro-protective effects on HIE based on $CoCl_2$-induced PC12 cell model in vitro and the neonatal rat hypoxic-ischemic (HI) brain damage model in vivo as well as try to illuminate the potential mechanism. This study may provide a new therapeutic drug for HIE.

Materials and Methods

Animal

Sprague-Dawley (SD) rats (200–250 g) were provided by the Laboratory Animal Center of the Wenzhou Medical University. They were raised under a 12 h light/dark cycle at temperature of 23°C ± 2°C and relative humidity of 60% ±10%. Water and food were provided ad libitum. This study was approved by the Wenzhou Medical University's Animal Care (wydw2024-0166) and Use Committee, and was performed in accordance with the Guide for the Care and Use of Laboratory Animals.

Establishment of HI Brain Damage Model and Pro Administration

To eliminate variations across pups, each litter was randomly divided into three groups, and the sample size was calculated according to a power analysis approach: Sham (n = 12), HI (n = 13), and HI+ Pro (n = 13). At least three independent replication experiments were performed. Using the standard = RAND () function generated random numbers. Neonatal rat hypoxic-ischemic brain damage (HIBD) models were established according to the modified Vannucci model.[33] Briefly, 7-day-old (P7) male pups were sedated with 100% ether and the left common carotid artery was rapidly separated and ligated after an incision in the center of the neck. The arteries between the two lymph nodes were cut, the tissues were reset, the skin incisions were sutured, and the wound was cleaned. After surgery, the pups were returned to their mothers for 2 hours of rest. They were then immersed in a humid gas mixture of 8% oxygen and 92% nitrogen at temperature of 37.5°C for 2.5 h at a gas flow rate of 3L/min. In the Sham group, the left common carotid artery was not ligated or was hypoxic. The HI+ Pro group was intraperitoneally injected with Pro (4 mg/kg) after 1 h successful modeling, and the Sham operation and HI groups were injected with the same amount phosphate-buffered saline (PBS). The treatment was continued for 7 days until the pups were euthanized. The route of administration and dose selection of Pro were based on a previous study.[28] Brain tissues were collected 24 h and 7 days after HI injury to assess the neuroprotective effects of Pro in the acute and subacute phases.

Infarct Volume Measurement

The infarct volume was analyzed by 2,3,5-triphenyl tetrazolium chloride (TTC, Sigma-Aldrich, St, MO, USA) staining. The brain tissues of rats in each group were collected 24 h after HIBD, frozen at −80°C for 5 min, and cut into 2 mm coronal slices. The samples were incubated in 1% TTC solution at 37°C in the dark for 30 min and then were immersed in 4% paraformaldehyde for 24 h. The infarct volume was calculated using ImageJ software (National Institutes of Health, MD, USA).

Brain Water Content Evaluation

To measure the degree of cerebral edema, brain tissues were harvested 24 h after HIBD in each group, and then the left (ie, wounded) hemispheres were separated and weighed to obtain the wet weight. The tissues were then dried for 72 h in an electrothermal oven at 70°C and weighed to obtain their dry weight. The percentage of brain water content was calculated using the following formula {(wet weight - dry weight)/wet weight] × 100%.

Hematoxylin and Eosin (HE) Staining and Nissl Staining

7 days after HIBD, the rats were severely sedated and 20 mL of sterile normal saline was injected into the heart, followed by reperfusion with an equal volume of 4% paraformaldehyde. Subsequently, the Brain tissues were collected and marinated in 4% paraformaldehyde at 4°C for 24 h. Paraffin-embedded sections were cut at a thickness of 5μm. The sections were dewaxed and stained with hematoxylin-eosin (H&E) (G1120, Solarbio, Beijing, China) or Nissl (G1432, Solarbio, Beijing, China) before being permeabilized in xylene. The sections were then sealed with a neutral resin. Finally, the tissue morphology was observed using an optical microscope (Nikon, Tokyo, Japan). The results were analyzed using ImageJ software.

Immunofluorescence Staining

Paraffin sections of brain tissue were collected from rats 24 h after HIBD, dewaxed, dehydrated, and heated in citrate buffer for antigen repair. For in vitro experiments, PC12 cells in each group were treated with $CoCl_2$ for 24 h on climbing slides and fixed with 4% PFA solution for 1 h. Samples of cells or brain tissue sections were permeabilized with 0.3% Triton X-100 (Sigma-Aldrich, MO, USA) for 30 min, rinsed with PBS, and blocked with 5% goat serum for 1 h at room temperature. Then, theses samples were incubated with primary antibodies (listed in Table S1) overnight at 4°C. The following day were incubated with fluorescently labeled secondary antibodies (1:200, Proteintech, CA, USA) for 1 h at 37°C and washed three times with PBS. The cells were stained with DAPI (S2110, Solarbio, Beijing, China) in the dark for 6 min. Finally, samples were examined under an inverted fluorescence microscope (Nikon, Tokyo, Japan).

TUNEL Assay

TUNEL labeling was performed on the brain tissues of each group using a TUNEL Apoptosis Detection Kit (40307ES20, Yeasen Biotechnology, Shanghai, China) to examine apoptosis. Briefly, paraffin sections of brain tissues 24 h after HIBD were dewaxed and dehydrated with an alcohol gradient, and then permeabilized with 20 μg/mL Proteinase K solution for 20 min. The cells were then incubated with TdT incubation buffer for 1 h at 37°C in a humid dark environment. Finally, the nuclei were stained with DAPI (S2110, Solarbio, Beijing, China), and images were taken using an inverted fluorescence microscope.

Cell Culture and Treatment

The Chinese Academy of Sciences Cell Bank (Shanghai, China) provided the differentiated PC12 cells. PC12 cells were maintained in dulbecco's modified Eagle's medium (DMEM, Gibco, United States) containing 10% fetal bovine serum (FBS, Gibco, NY, USA) at a 37°C, 5% CO_2 incubator. $CoCl_2$ (C8661, Sigma-Aldrich, St. Louis, MO, USA) was used to induce simulated cell hypoxia, which is known to induce the production of 72 reactive oxygen species.[34] Pro and AMPK inhibitor Compound C (CC, MCE, NJ, USA) were dissolved in DMSO to prepare the reserve solution. Based on our preliminary concentration gradient experiments, 1 mm (Cell viability was closest to 50%) $CoCl_2$ and 20 μM (maximum cell viability) Pro were selected as optimal working concentrations for the cells. We set up different groups such as Control, $CoCl_2$, $CoCl_2$+Pro, $CoCl_2$+ CC, $CoCl_2$+Pro+CC. PC12 cells were treated with $CoCl_2$ or CC (2.5 μM) in advance and then supplemented with Pro, CC, or a mixture of Pro and CC for 24 h. Finally, these cells were used for subsequent experiments. Cells in the Control group were incubated in culture medium containing DMSO (0.1% v/v).

Cell Viability Assay

The cell viability of each group was determined using the CCK-8 Kit (Yeasen, Shanghai, China). PC12 cells at a density of 1×10^4 cells/well were seeded in 96-well plates and cultured in media containing different concentrations of $CoCl_2$ or Pro for 24 h at a 37°C, 5% CO_2 incubator. Subsequently, 10% volume of CCK-8 solution was added to each well, then the plate was incubated at 37°C for 40 min in the dark. The optical density (OD) of the reaction solution was measured at 450 nm using a microplate reader (Thermo, MA, USA), and the results were compared with the control group to obtain the cell survival rate.

Oxidative Stress Evaluation

Oxidative stress was evaluated by quantifying the levels of malondialdehyde (MDA) (Solarbio, Beijing, China) and Catalase (CAT) (Solarbio, Beijing, China) using commercially available kits. Briefly, in vivo, equal weights of the left cerebral hemispheres were collected from each group 24 h after HIBD, and for in vitro, the same number of cells was collected from each group. Tissue homogenates were prepared by adding the extract liquid to the brain tissue or cells and centrifuging at 8000×g for 10 min at 4°C to collect the supernatant. Finally, the activities and levels of various oxidative stress markers were measured according to the manufacturer's instructions.

Measurement of Reactive Oxygen Species (ROS)

In living cells, ROS is produced under stimuli such as hypoxia, serum deprivation, or cytokine stimulation.[33] In vitro, intracellular ROS levels were detected using a DCFH-DA probe (Beyotime, Shanghai, China). Briefly, cells were incubated with 10 μM DCFH-DA at 37°C in the dark for 30 min, then washed three times with serum-free cell culture medium. Subsequently, the cells were digested and harvested. Finally, the collected cells were examined for labeled cells by flow cytometry (Beckman, CA, USA).

Mitochondrial ROS Detection

Mitochondria are the main intracellular organelles that produce ROS.[8] Therefore, we used the mitochondrial superoxide anion fluorescent indicator MitoSOX Red Reagent Assay Kit (Yeasen, Shanghai, China) to detect mitochondrial ROS levels. In brief, PC12 cells in each group were washed with Hank's balanced salt solution (HBSS), and then 5 μM

MitoSOX Red was added to each group to fully cover the growing cells. The cells were incubated at 37 ° C in the dark for 30 min, washed 3 times with PBS, fixed with methanol for 10 min, and placed on slides. Finally, the nuclei were stained with DAPI, and cell morphology was observed under a Ni-U fluorescence microscope.

Annexin V and PI Assay

The Annexin V FITC/PI Apoptosis Detection Kit (BD, NJ, USA) was used to assess the early and late apoptotic activities of the cells in each group. Briefly, cells were harvested by digestion with 0.25% ethylenediaminetetraacetic acid (EDTA) trypsin (25200072, Gibco, Grand Island, NY, United States) and then resuspended in Binding Buffer after washing twice with PBS. The cells were further stained with a mixture of 5μL of FITC Annexin V and 5μL of PI in the dark at room temperature for 15 min. Finally, positive and negative controls were used to determine the flow cytometry (Beckman, CA, USA) threshold for detecting cell apoptosis rates according to the kit instructions.

Western Blot Analysis

Proteins were prepared from homogenized brain proteins and PC12 cells in each group using RIPA buffer (Solarbio, Beijing, China) containing phenylmethyl-sulfonyl fluoride (PMSF, Solarbio, China) and a phosphatase inhibitor (P1260, Solarbio, Beijing, China), and centrifuged at 13,200×g and 4°C for 30 min to harvest supernatant. The protein concentration was determined using a BCA Protein Assay Kit (Beyotime, Shanghai, China). Protein samples (40 μg each) were separated by electrophoresis on sodium dodecyl sulfate (SDS)-polyacrylamide separation gels and then transferred to PVDF membranes. Membranes were blocked with 5% non-fat milk for 2 h at room temperature and then were incubated with primary antibodies (listed in Table S1) overnight at 4°C. Membranes were then incubated with a 1:1000 dilution of rabbit or mouse secondary antibodies conjugated to horseradish peroxidase (Beyotime, Shanghai, China) for 2h at room temperature and washed three times for 10 min each. Finally, the membranes were exposed to enhanced chemiluminescence (ECL) reagents (Amersham, IL, USA) and the protein bands were visualized using a ChemiDoc XRS Imaging System (Bio-Rad, CA, USA). Image J was used to quantify the signal intensity of each protein band. The band intensities of target proteins in each group were compared according to the band intensity of a reference protein within each group, to correct for differences in protein loading between samples.

Statistical Analysis

For all experiments, data were collected from at least three independent experiments, and quantitative data were presented as mean ± standard deviation (SD). GraphPad Prism 8.0.2 statistical software (GraphPad Software Inc., CA, USA) was used for statistical analysis. The letter "n" in figure legends means the number of biological replicates, and "n" in text means the analyzed sample size. Inter-group comparisons by one-way analysis of variance, followed by Tukey's post hoc test when analyzing more than two groups. The Student's unpaired *t*-test was used for comparisons between two groups. Results were considered statistically significant if p-value was < 0.05, and $ns > 0.05$, which was not considered statistically significant.

Results

Pro Attenuated Acute Brain Injury in Neonatal Hypoxia-Ischemia (HI) Rats

The chemical structure of the pro (Figure 1A) and timeline of the experimental design for the in vivo experiment (Figure 1B) are shown in this study. To investigate whether Pro could reduce acute brain injury, TTC staining was used to evaluate rat brain infarction in the Sham, HI, and HI + Pro groups (Figure 1C). The quantitative results of TTC staining showed that there was no infarct in the Sham group, and compared with the HI group, Pro treatment significantly reduced the volume of cerebral infarction (Figure 1D). In addition, edema was evident on the left side of rats in the HI group compared to the Sham group, and Pro treatment significantly reduced HI-induced ipsilateral cerebral edema in rats (Figure 1E). The quantitative results of brain water content showed the same trend (Figure 1F). These results suggest that Pro intervention effectively alleviated acute brain injury in neonatal HI rats.

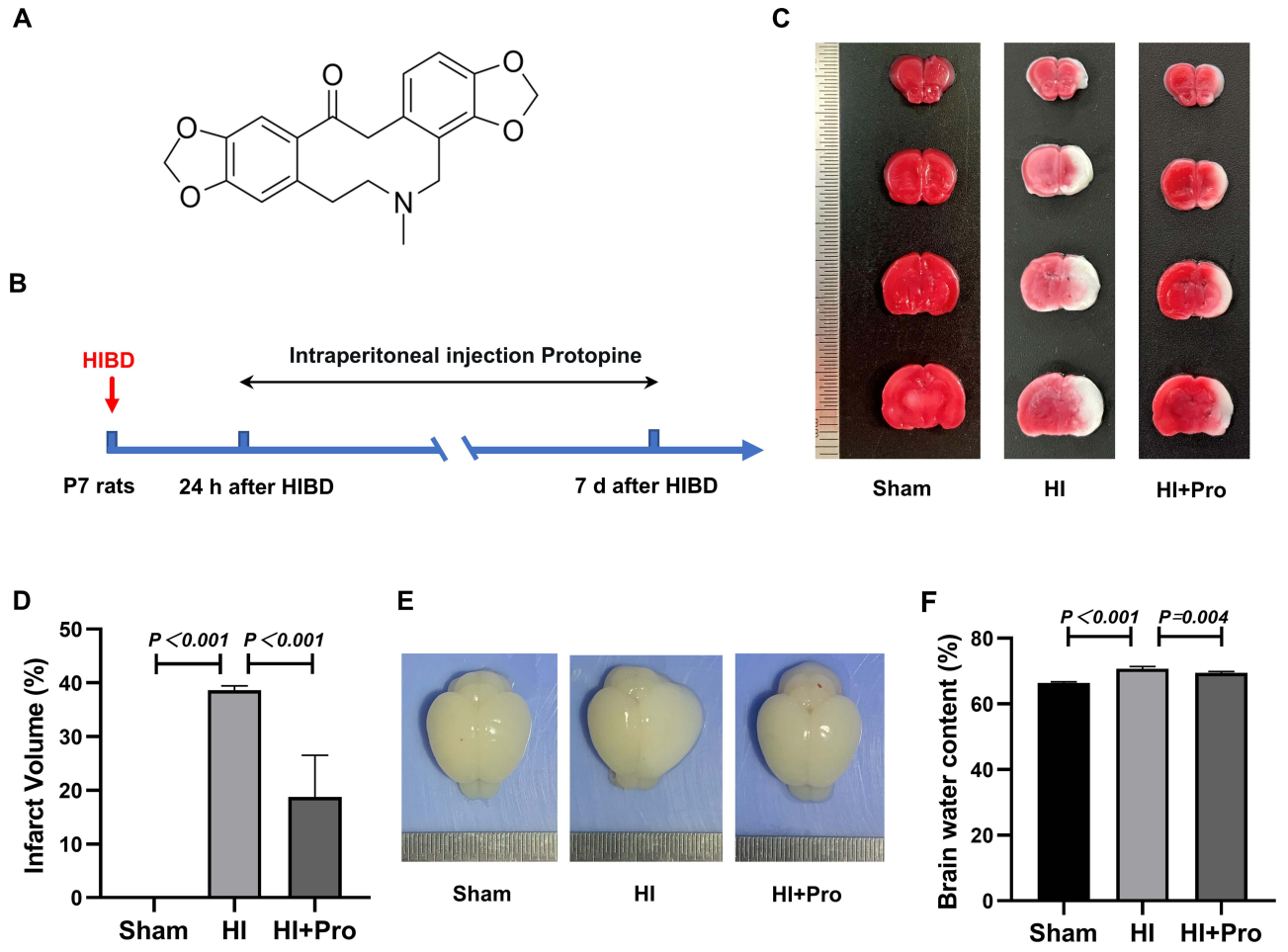

Figure 1 Pro treatment attenuated acute hypoxia-ischemia (HI) brain injury in neonatal rats. (**A**) The chemical structure of protopine. (**B**) The timeline of in vitro experiments. (**C**) The representative images of TTC staining of Coronal brain sections 24 h after HI brain injury (n = 4). Scale bar: 0.5 mm. (**D**) Calculation of the infarct volume depicted by TTC staining. All data are presented as mean ± SD. (n = 4). (**E**) Representative images of the brain from each group 24 h after HI brain injury (n = 4). Scale bar: 0.5 mm. (**F**) The ratio of wet and dry in each group (n = 5). The data are presented as mean ± SD.

Pro Treatment Inhibited White Matter Damage and Microglial Activation in HI-Induced Rats

Microtubule-associated protein 2 (MAP2) functions as a somatic dendritic marker and is a key cytoskeletal regulator in neuronal dendrites.[35] Ischemia can disrupt cytoskeleton integrity of the cytoskeleton.[36] Oligodendrocytes are mainly found in the brain and spinal cord. The proper structure of oligodendrocyte myelin is dependent on several proteins, including myelin basic protein (MBP).[37] Western blot was performed to detect the expression of MAP-2 and MBP in the brain to investigate the effect of Pro on myelin regeneration and axonal repair in HI rats (Figure 2A). Compared with the Sham group, the levels of MAP-2 and MBP were significantly downregulated in the HI group, although Pro treatment rescued this trend (Figure 2B). To further study the effect of Pro on microglial activity, we performed immunofluorescence staining for the molecular marker of microglia, ionized calcium-binding adapter molecule 1 (IBA-1) (Figure 2C). The results showed that the expression of IBA-1 in the cerebral cortex or DG region of the hippocampus significantly increased after HI injury, indicating that the microglia in these two regions were significantly enlarged and densely distributed as the number of cell branches increased. Moreover, Pro intervention significantly reduced IBA-1 expression, blocked microglial activation, and decreased the number of cell branches in the HI-induced rats (Figure 2D). To further explore the neuroprotective effects of Pro, the anatomy of the brain in each group was observed 7 days after HI (Figure 2E). Quantitative results revealed a greater necrotic volume in the brain in the HI group than in the Sham group, and Pro treatment reduced the cerebral infarction caused by hypoxia and ischemia (Figure 2F).

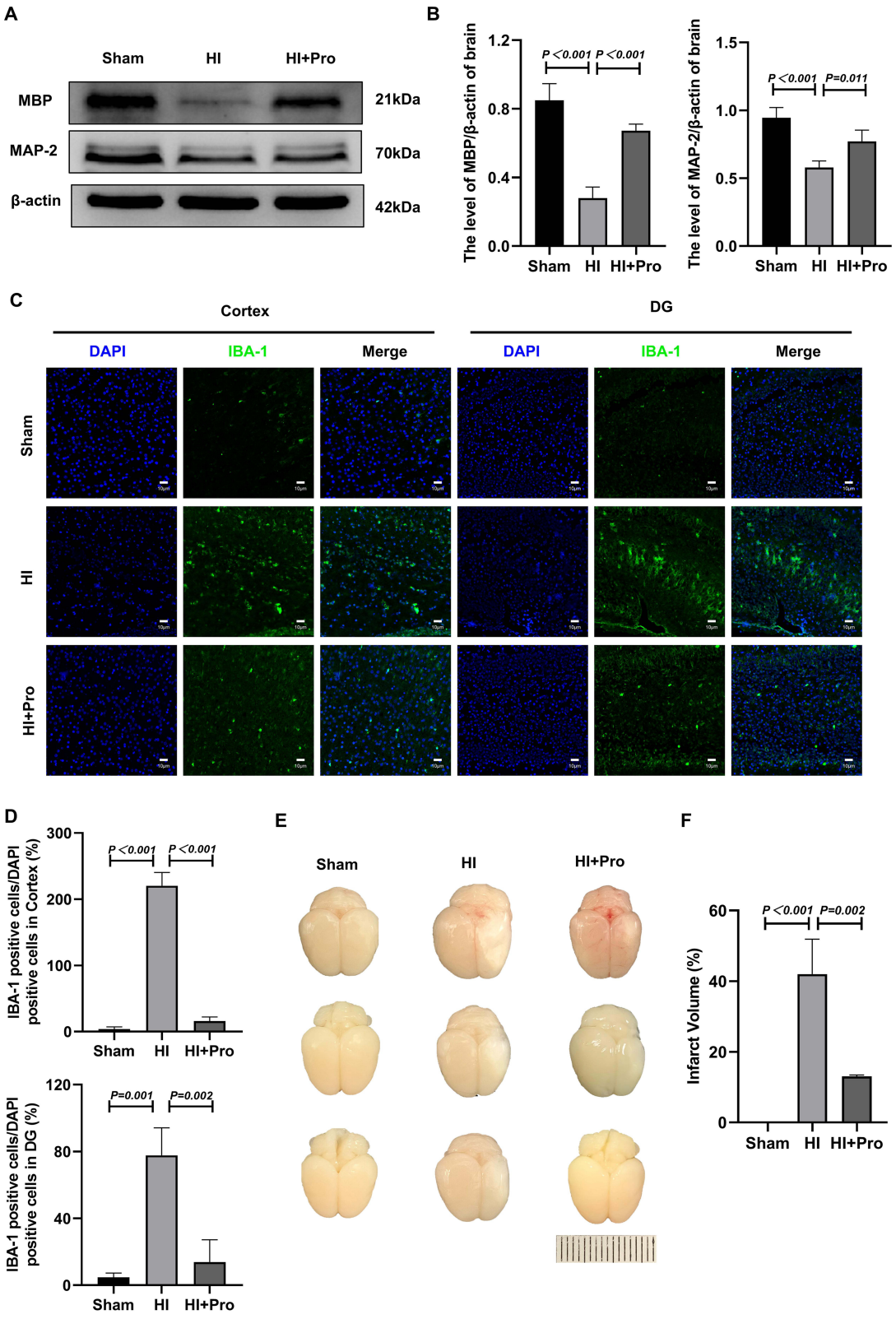

Figure 2 Pro treatment inhibited white matter damage and microglial activation after hypoxic-ischemic (HI) brain injury in neonatal rats. (**A**) The protein levels of MAP and MBP expression by Western blot 7 days after HI brain injury. (**B**) Analyses of MAP and MBP (n = 4). (**C**) Representative immunofluorescence staining images of IBA-1 (green) and DAPI (blue) on the brain tissues. Scale bar = 10 μm. (**D**) The ratio of IBA-1 positive cells (of all cells) (n = 3). (**E**) Representative images of the brain from each group 7 days after HI injury (n = 5). Scale bar: 0.5 mm. (**F**) Ratio of the injured hemisphere to the contralateral hemisphere. The data are presented as mean ± SD.

https://doi.org/10.2147/DDDT.S484969 DovePress

Pro Alleviated the Brain Tissue Structural Damage Caused by HI

The protective effect of Pro on neurons was evaluated using whole-brain Nissl and H&E staining. Compared with the Sham group, Nissl bodies were almost absent in the cerebral cortex and hippocampal CA1, CA3, and DG regions in the HI group, but more Nissl bodies appeared around the nucleus after Pro intervention (Figure 3A). HE staining revealed that the HI group suffered significant damage in the cerebral cortex and hippocampal CA1, CA3, and DG regions as well as disrupted neuronal organization, cell shrinkage, and nuclear chromatin condensation, while the HI group had fewer normal neurons than the other groups (Figure 3B). The number of neurons in the hippocampal CA1, CA3, and DG regions was counted, and it was discovered that HI damage caused a considerable reduction in the number of cells in the CA1, CA3, and DG regions; however, Pro treatment increased the number of normal neurons and restored the cell structure (Figure 3C).

Pro Reduced Apoptosis and Oxidative Stress and Further Activated AMPK/PGC1α Pathway

To explore whether Pro could reduce neuronal apoptosis after HI brain damage in rats, TUNEL staining of the cortex and hippocampal CA1 region was performed (Figure 4A). The results showed that compared with the Sham group, there was a significant increase in TUNEL-positive cells in the cerebral cortex and hippocampal CA1 area in the HI group, although Pro intervention dramatically reduced the number of TUNEL-positive cells (Figure 4B). In addition, Western blotting was used to identify the expression of the apoptosis protein BAX and anti-apoptotic protein BCL-2 in each group (Figure 4E). Quantitative findings indicated that compared to the sham group, the expression of BAX was greatly upregulated and the expression of BCL-2 was significantly downregulated in the HI group, and Pro treatment reversed these trends in HI-induced rats (Figure 4F). To explore the effect of Pro on oxidative stress after HIBD, we assessed the MDA (Figure 4C) and CAT levels (Figure 4D) in each group. The MDA content in the HI group was significantly higher than that in the Sham group, and Pro significantly reduced MDA levels. The CAT level was observably decreased in the HI group, but Pro treatment significantly reversed this trend in HI-induced rats. These findings suggest that Pro ameliorates HI-induced brain damage by inhibiting apoptosis and oxidative stress. Western blotting was performed to examine the protein expression of AMPK, PGC1α, NRF1, and TFAM in the different groups (Figure 4G). The quantitative results showed that the levels of p-AMPK and PGC1α in the HI group were higher than those in the Sham group, and Pro administration further upregulated these protein levels in HI-induced rats. Pro treatment also increased NRF1 and TFAM expression in HI-induced rats, which depended on activation of the AMPK/PGC1α pathway (Figure 4H). These findings indicated that Pro may play a neuroprotective role in HI rats by activating the AMPK/PGC1α pathway to regulate NRF1/TFAM in a positive feedback manner.

Pro Attenuated $CoCl_2$-Induced ROS Production and Apoptosis in PC12 Cells

We used $CoCl_2$-induced PC12 cells were used to simulate HI in vitro. $CoCl_2$ competes with the oxygen in the medium to reduce the oxygen partial pressure and simulate an anoxic environment. Based on the cell viability analysis using CCK-8, the optimal concentration of $CoCl_2$ (1000 μM) was selected (Figure S1A). The harmful effects of the medicines were eliminated (Figure S1B) and the optimal working concentration of Pro was determined to be 20 μM (Figure S1C).

In addition, MitoSOX fluorescent probe staining was conducted to analyze the mitochondrial ROS levels in each group (Figure 5A). Quantitative results showed that ROS production in PC12 cells increased significantly after $CoCl_2$ induction, whereas ROS production decreased significantly after Pro intervention (Figure 5B). In addition, Pro intervention downregulated CAT content (Figure 5C) and decreased MDA levels (Figure 5D) in $CoCl_2$ induced PC12 cells. Annexin V and PI co-staining were used to determine apoptosis in each group (Figure 5F). Annexin V-positive cells indicate early apoptotic cells, whereas Annexin V and PI positivity indicate late apoptotic cells. Quantitative findings revealed that there were essentially no Annexin V or PI positive cells in the Control group, but Pro was able to considerably suppress the increase in Annexin V or PI positive cells generated by $CoCl_2$ (Figure 5E). These findings indicated that Pro may reduce $CoCl_2$-induced PC12 cell damage by decreasing mitochondrial ROS generation and apoptosis.

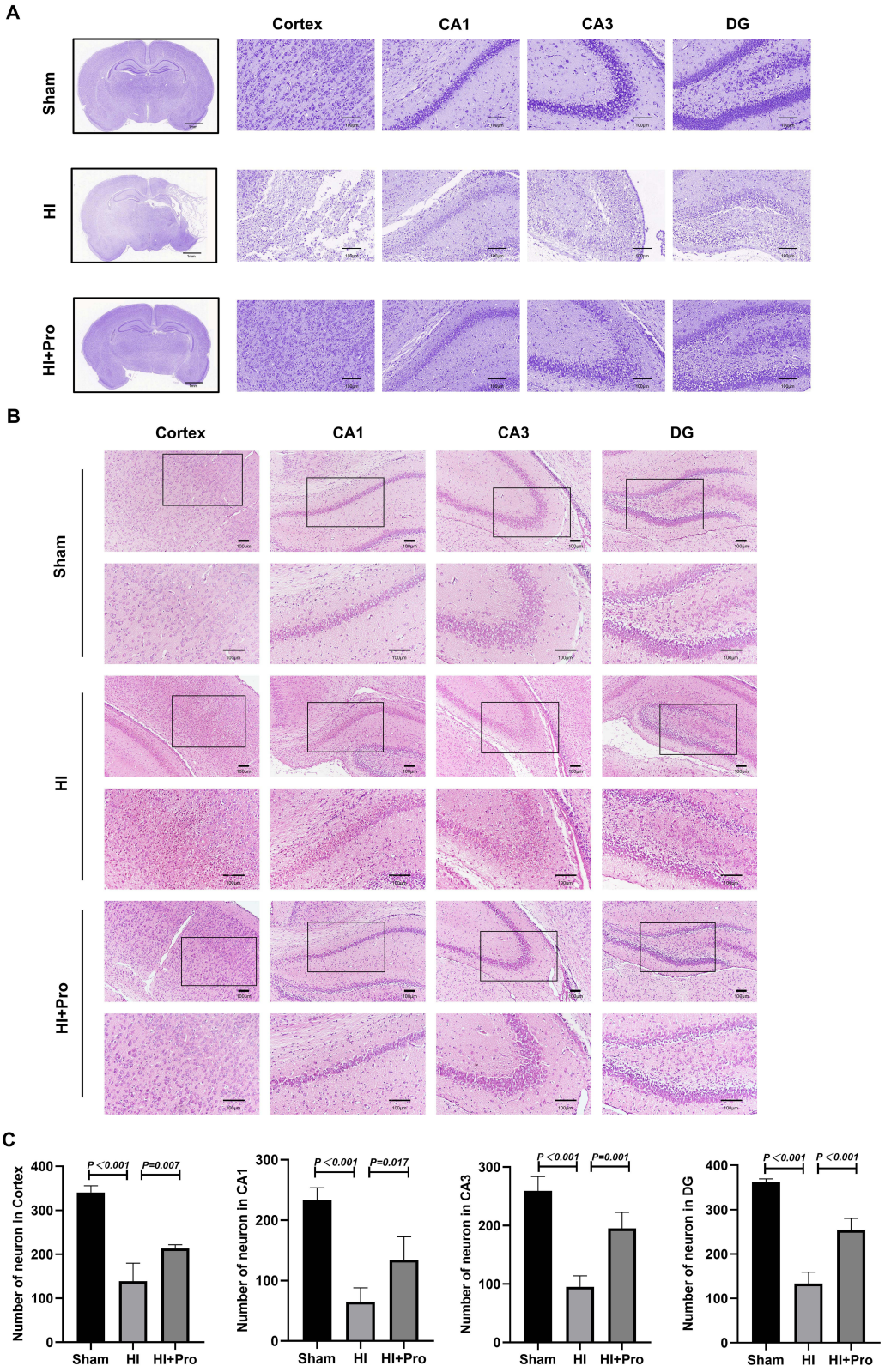

Figure 3 Pro ameliorated the tissue structural damage and reduced the loss of neurons. (**A**) Representative image of Nissl staining 7 days after HI brain injury. Scale bar = 100 μm. (**B**) Representative image of HE staining in the cortex, hippocampal CA1, CA3, and DG region 7 days after HI brain injury. Scale bar = 100 μm. (**C**) Quantification analysis of neuron numbers in brain cortex, hippocampal CA1, CA3, and DG region (n = 4). The data are presented as mean ± SD.

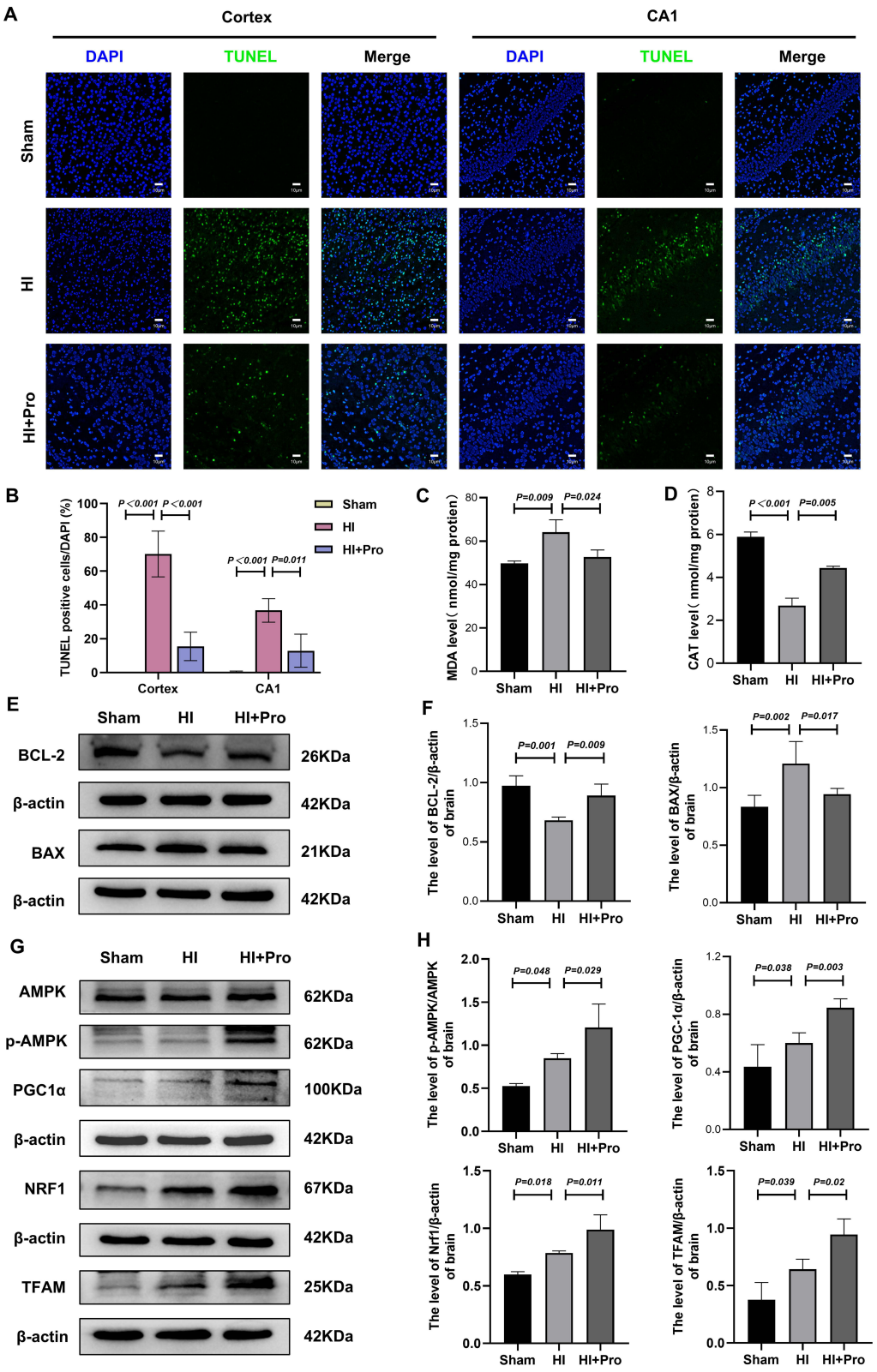

Figure 4 Pro treatment suppressed apoptosis and oxidative stress caused by HI brain damage and exerted neuroprotection via the AMPK/PGC1α pathway to activate NRF1/TFAM in positive feedback manner. (**A**) Representative immunofluorescence staining images of TUNEL (green) and DAPI (blue) in brain cortex and CA1 24 h after HI brain injury. Scale bar = 10 μm. (**B**) Quantitative analysis of TUNEL-positive cells in Cortex and hippocampal CA3 region (of all cells) (n = 3). (**C**) The MDA level in brain tissues 24 h after HI brain injury (n = 3). (**D**) The CAT level in brain tissues 24 h after HI brain injury (n = 3). (**E**) The protein levels of BCL-2 and BAX expression by Western blotting in brain tissues. (**F**) Analyses of BCL-2 and BAX (normalized to β-actin) (n = 4). (**G**) The protein levels of AMPK, p-AMPK, PGC1α, NRF1 and TFAM expression by Western blotting in brain tissues. (**H**) Analyses of AMPK, p-AMPK, PGC1α, NRF1 and TFAM (normalized to β-actin) (n = 4). The data are presented as mean ± SD.

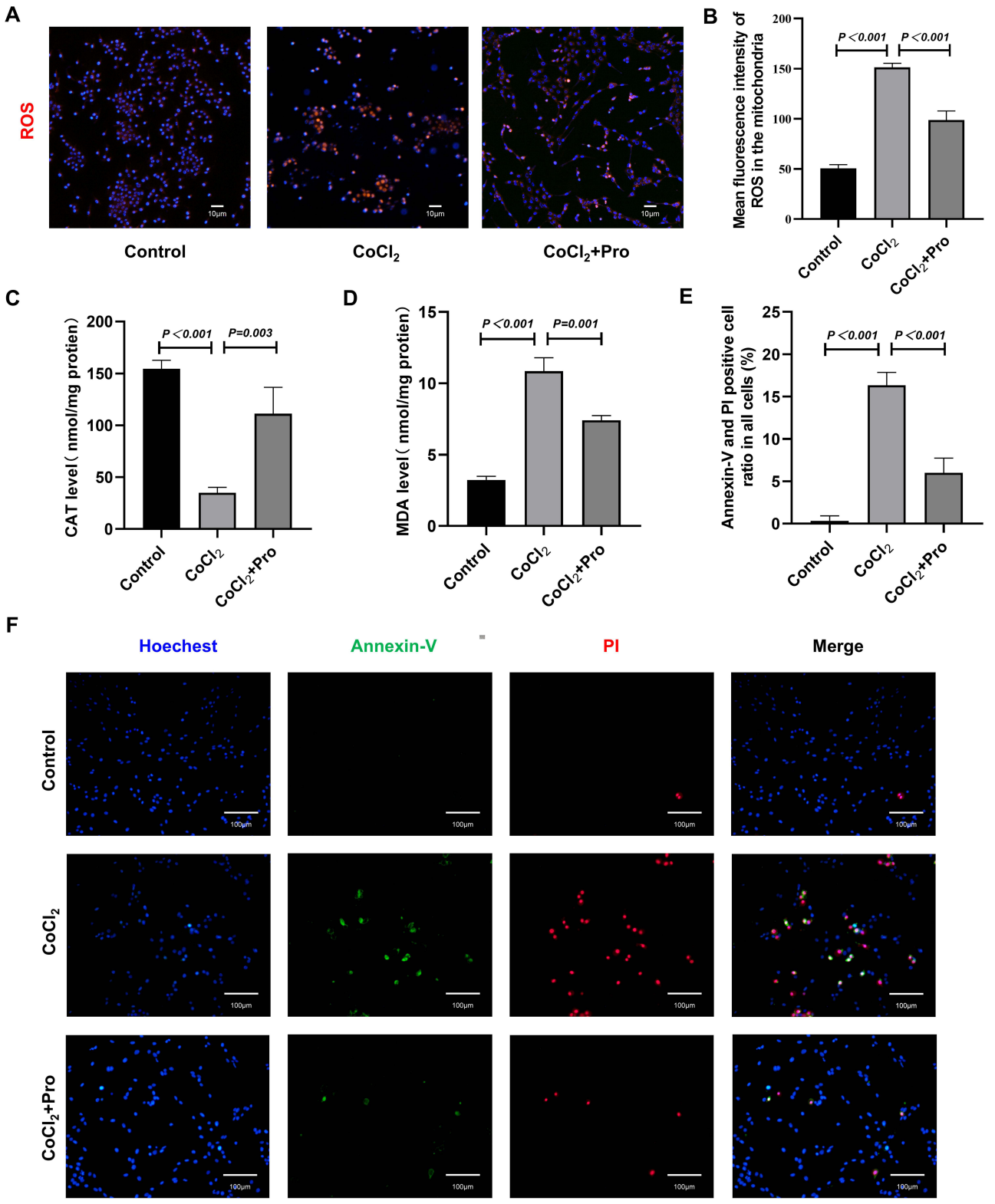

Figure 5 Pro attenuated $CoCl_2$-induced oxidative stress damage and apoptosis in PC12 cell. (**A**) The mitochondrial ROS generation of PC12 cell was detected by MitoSOX (red) and DAPI (blue) staining (n = 3). Scale bar: 10 μ m. (**B**) Mean fluorescence intensity of ROS in the mitochondria of PC12 cells after $CoCl_2$ injury (n = 3). (**C**) The CAT level in PC12 cells after $CoCl_2$ injury (n = 3). (**D**) The MDA level in PC12 cells after $CoCl_2$ injury (n = 3). (**E**) Quantitative analysis of Annexin V and PI positive cells (n = 3). The data are presented as mean ± SD. (**F**) Representative immunofluorescence staining images of Annexin V FITC (green), PI (red) and Hoechest (blue) in PC12 cells after $CoCl_2$ injury. Scale bar: 100 μm.

https://doi.org/10.2147/DDDT.S484969 DovePress

Inhibition of AMPK Reversed the Anti-Oxidative Stress and Anti-Apoptosis Effects of Pro

To further explore the protective mechanism of Pro against $CoCl_2$-induced PC12 cell injury, the AMPK inhibitor, CC, was used to detect oxidative stress and apoptosis in each group. A MitoSOX fluorescent probe was used to stain ROS in mitochondria (Figure 6A). The results showed that Pro significantly reduced ROS levels in $CoCl_2$-induced PC12 cells, but this effect was reversed by CC treatment (Figure 6B). The intracellular ROS levels in each group were detected by flow cytometry using DCFH-DA fluorescence staining (Figure 6C). The quantitative results showed that Pro intervention could significantly reduce the ROS level in $CoCl_2$-induced PC12 cells, similarly, CC could reverse the effect of Pro on $CoCl_2$-induced PC12 (Figure 6D). In addition, the expression of BAX and BCL-2 apoptosis-related proteins in each group was detected using Western blotting (Figure 6E). The quantitative results indicated that $CoCl_2$ considerably increased the expression of BAX and decreased the expression of BCL-2, which could be significantly reversed by Pro therapy. However, the effect of Pro combined with CC was relatively weakened (Figure 6F). Flow cytometry was performed to detect apoptosis in each group using Annexin V and PI co-staining (Figure 6G). The percentage of early apoptotic cells (Q3) and late apoptotic cells (Q2) was calculated. These quantitative results were consistent with the ROS results (Figure 6H). These results further suggest that Pro might attenuate $CoCl_2$-induced cellular oxidative stress and apoptosis by activating the AMPK pathway.

Pro Alleviated $CoCl_2$-Induced PC12 Injury Through AMPK/PGC1α Pathway to Activating NRF1/TFAM

The effects of Pro on the AMPK/PGC1α pathway expression were assessed by Western blotting in vitro (Figure 7A). The results showed that compared with the Control group, the expression of p-AMPK, PGC1α, NRF1, and TFAM were upregulated in the $CoCl_2$ group. However, Pro treatment further enhanced the levels of p-AMPK, PGC1α, NRF1, and TFAM compared to those in the $CoCl_2$ group. In contrast, the Pro + CC group had significantly lower levels of p-AMPK, PGC1α, NRF1, and TFAM than the Pro group (Figure 7B). In addition, consistent with the Western blotting results, similar changes in PGC1α and TFAM expression in PC12 cells were confirmed by immunofluorescence staining (Figure 7C–F). These data further demonstrated that Pro might alleviate $CoCl_2$-induced PC12 injury through the AMPK/PGC1α pathway to activate NRF1/TFAM.

Based on the above results, we speculate that Pro may play a neuroprotective role by further activating the AMPK/PGC1α pathway to regulate the NRF1/TFAM transcription factor, thereby reducing oxidative stress and apoptosis. A detailed diagram illustrating the potential mechanism by which Pro exerts neuroprotective effects against HI injury is shown in Figure 8.

Discussion

HIE is caused by insufficient blood and oxygen supplies due to perinatal asphyxia. At present, hypothermia is a standard treatment method for HIE, but it has limited effects on patients with moderate and severe injuries, and the treatment time window is narrow.[38,39] Therefore, there is an urgent need to search for more effective therapeutic drugs for HIE. The previous study has confirmed oxidative stress and apoptosis are involved in HIE pathological injury.[9] In this study, we tried to investigate the neuroprotective effects of Pro on HI brain damage in vitro and in vivo and illuminate the potential mechanism.

Pro is an alkaloid found in various plants that has been shown to have a variety of pharmacological effects. In the nervous system, Pro plays an essential role in good permeability and can pass through the blood-brain barrier, effectively promoting the degradation of neurofibrillary plaques formed by tau in the cells of patients with Alzheimer's patients.[26] But the underlying molecular mechanisms of the neuroprotective effects of Pro are not fully understood. Alam et al found that Pro inhibits neuroinflammation in lipopolysaccharide (LPS)-induced BV2 cells through the MAPK/NF-κB pathway.[19] However, whether Pro exerts a neuroprotective effect on HI brain damage remains unclear.

In the present study, the Vannucci method was used to establish a neonatal rat model of HI brain damage to study the neuroprotective effects of Pro in vivo. Our results showed that Pro effectively improved brain edema and

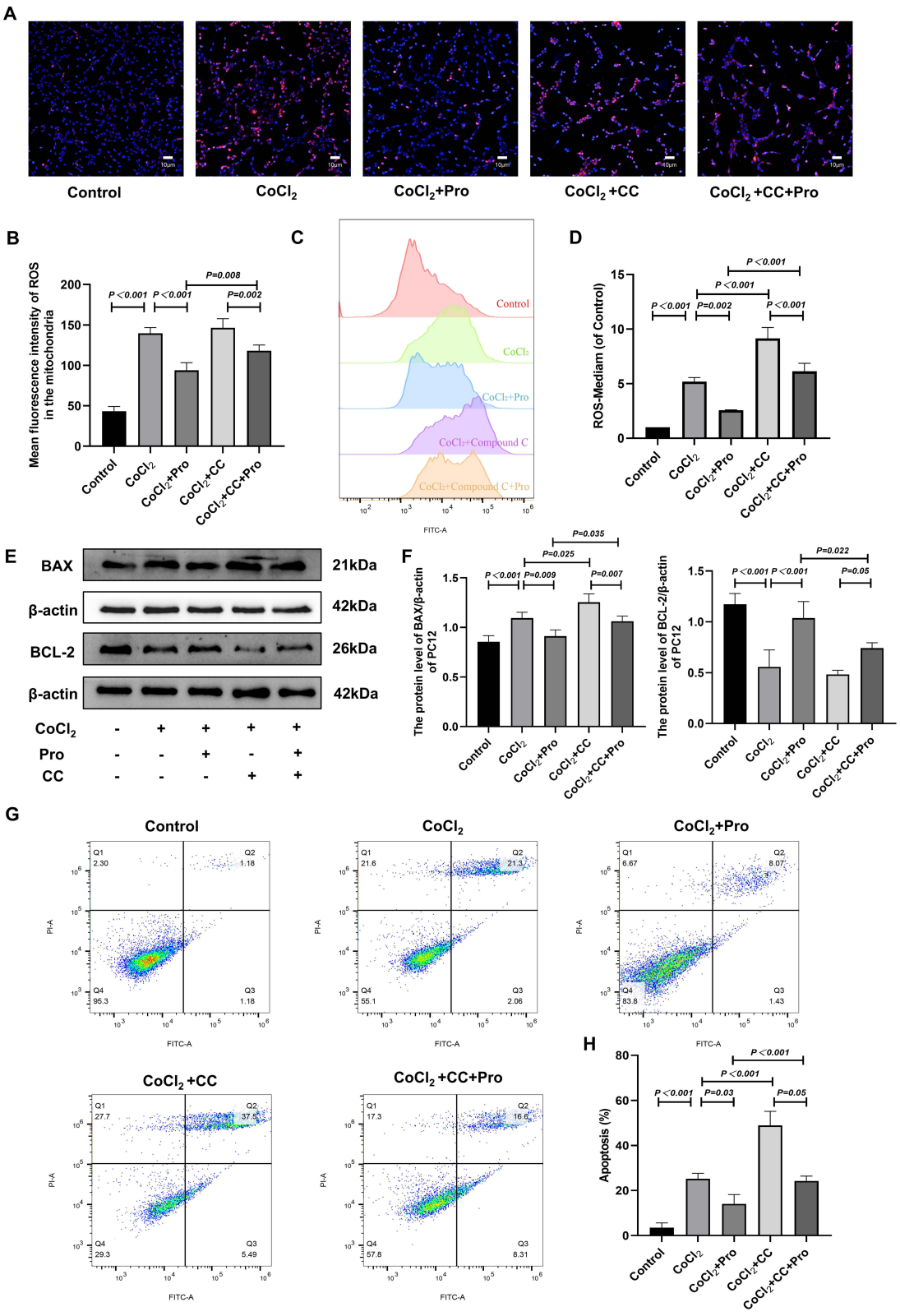

Figure 6 CC reversed the neuro-protective effect of Pro after $CoCl_2$-induced injury in PC12 cell. (**A**) The generation of mitochondrial ROS in each group was detected by MitoSOX (red) and DAPI (blue) staining of PC12 cells after $CoCl_2$ injury (n = 3). (**B**) Mean fluorescence intensity of ROS in the mitochondria of each group (n = 4). (**C**) Representative and pooled data showing ROS production using flow cytometry (n = 3). (**D**) Quantitative analysis of ROS generation in PC12 cells using flow of ROS (n = 3). (**E**) The protein levels of BCL-2 and BAX expression by Western blotting in PC12 cells after $CoCl_2$ injury (n = 4). (**F**) Analysis of BCL-2 and BAX levels (normalized to β-actin) (n = 4). (**G**) Apoptosis in each group was analyzed and quantified using Annexin V FITC and PI staining flow cytometry (n = 3). (**H**) Quantitative analysis of Annexin V FITC and PI staining flow cytometry (n = 3). The data are presented as the mean ± SD.

https://doi.org/10.2147/DDDT.S484969 DovePress

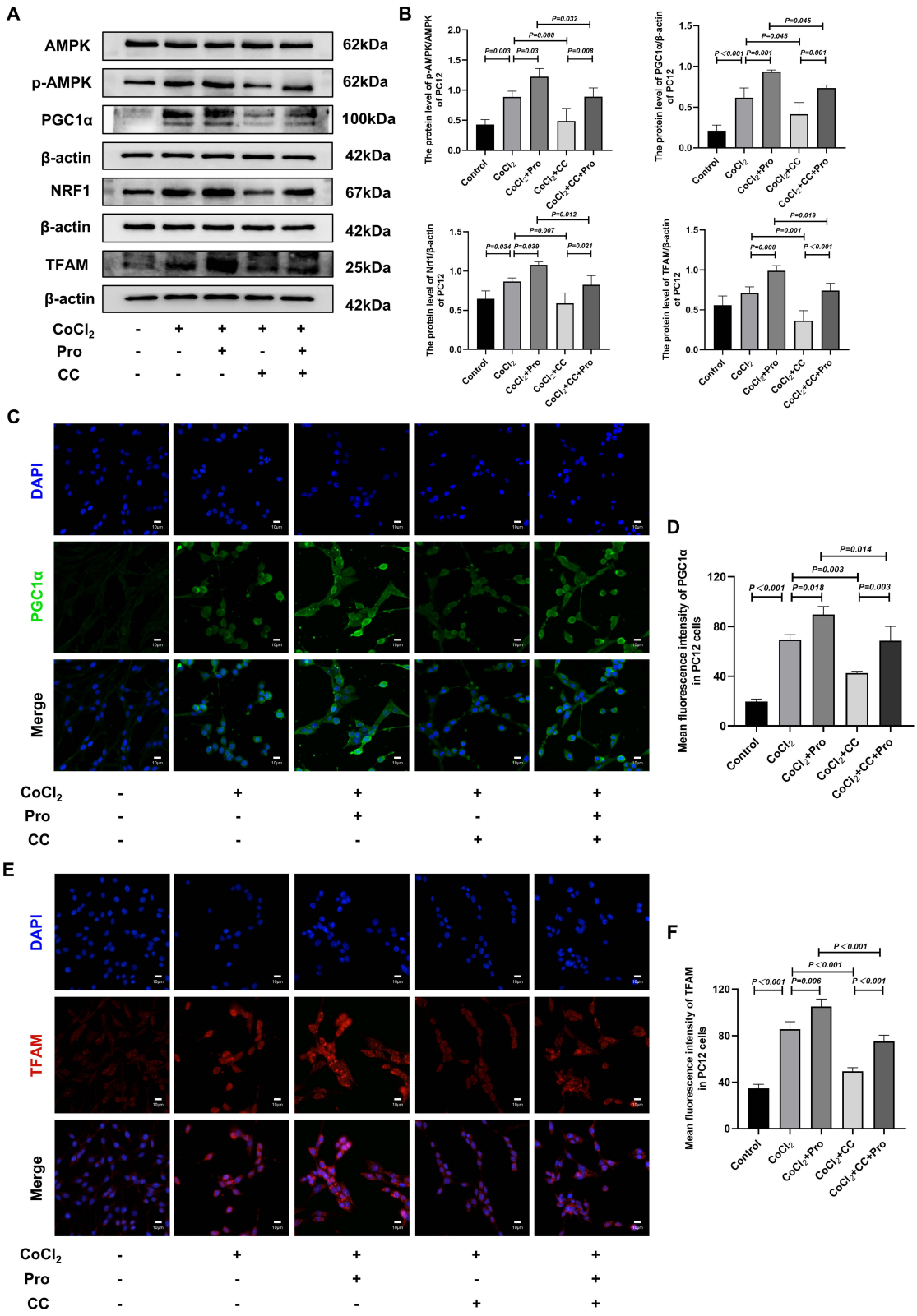

Figure 7 Pro exerted neuroprotection through activates AMPK/PGC1α pathway to regulate NRF1/TFAM transcription factor. (**A**) The protein levels of AMPK, p-AMPK, PGC1α, NRF1, and TFAM expression by Western blotting in PC12 cells after $CoCl_2$ injury (n = 4). (**B**) Analyses of AMPK, p-AMPK, PGC1α, NRF1 and TFAM (normalized to β-actin) (n = 4). (**C**) The representative immunofluorescence staining images of PGC1α (green) and DAPI (blue) in PC12 from each group (n = 4). Scale bar: 10 μm. (**D**) Quantitative analysis of Mean fluorescence intensity of PGC1α in PC12 cells (n = 4). (**E**) The representative immunofluorescence staining images of TFAM (red) and DAPI (blue) in PC12 from each group (n = 4). Scale bar: 10 μm. (**F**) Quantitative analysis of Mean fluorescence intensity of TFAM in PC12 cells (n = 4). The data are presented as mean ± SD.

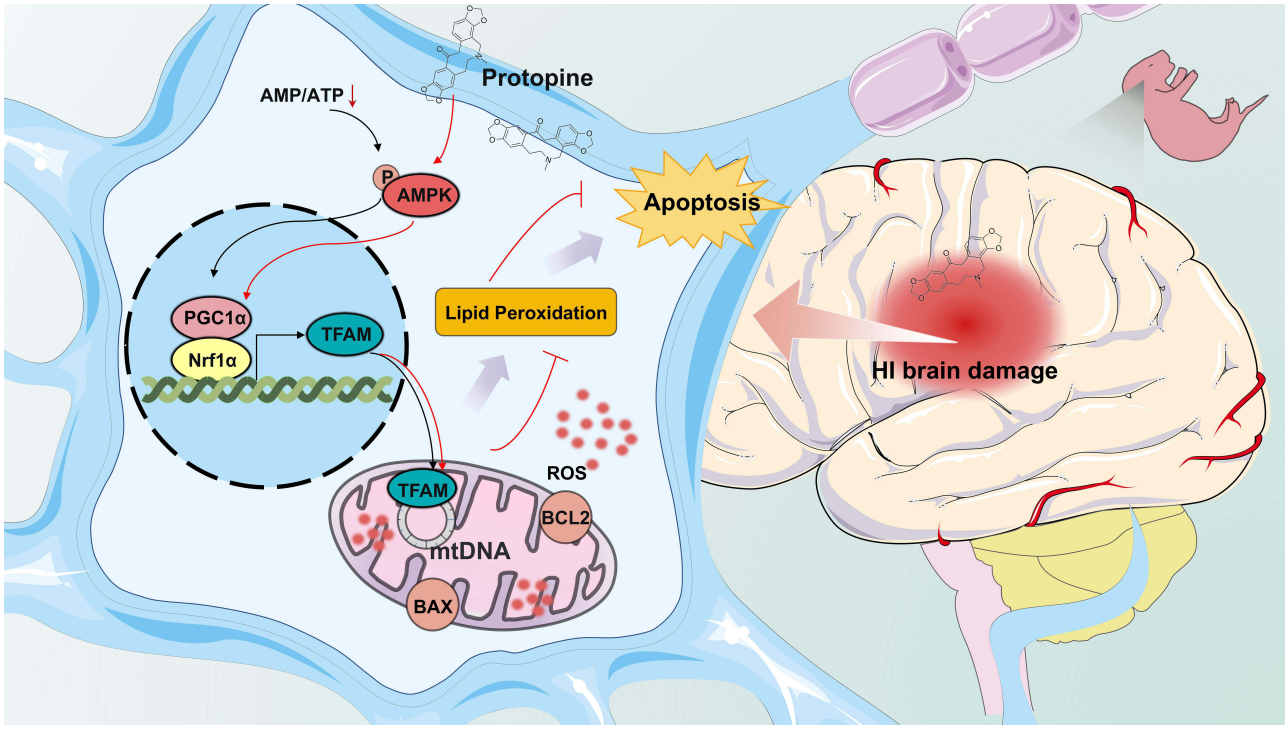

Figure 8 Pro improves the mechanism of action of HIE by activating AMPK/PGC1α pathway to activate NRF1/TFAM in positive feedback manner to inhibit oxidative stress damage and apoptosis.

histomorphology in neonatal HIBD rats. Pro also promotes the recovery of oligodendrocyte myelin by inhibiting the downregulation of MAP2 and MBP in HI-induced rats. Additionally, a $CoCl_2$-induced PC12 model was established to study the neuroprotective role of Pro in vitro. Our results showed that Pro promoted cell viability and reduced apoptosis and ROS production in $CoCl_2$-induced PC12.

HIE pathogenesis is complex. The neonatal brain is more susceptible to oxidative stress injury due to both high oxygen consumption and weak antioxidant capacity, which cause lipid peroxidation, protein oxidation, DNA destruction, and mitochondrial inhibition.[40,41] In our study, MitoSOX fluorescence staining and ROS flow cytometry results showed that both mitochondrial and total intracellular ROS levels were significantly increased after HI injury, whereas Pro intervention inhibited HI-induced ROS production. Moreover, ROS-induced lipid peroxidation, a free radical chain reaction that spreads rapidly, can affect a large number of lipid molecules and proteins and even cause loss of enzyme activity.[42] MDA, an indicator of lipid peroxidation, in HI-induced brain and $CoCl_2$-induced PC12 cells, but Pro treatment could significantly prevent the occurrence of lipid peroxidation. CAT, a core enzyme of the eukaryotic antioxidant system, was significantly decreased in HI in vivo and in vitro models; however, Pro intervention dramatically rescued this reduction. The excessive oxidative stress can activate mitochondrial apoptosis process.[43] In this study, Pro could effectively alleviate cell apoptosis induced by HI damage in vivo and in vitro through mitochondrial or total intracellular ROS.

Brain is a high energy-consuming organ that is very sensitive to ischemic stimuli, and energy stores can last only a few min in the absence of energy influx.[44] A decrease in the AMP/ATP ratio at low energy induces phosphorylation of AMPK, an early energy sensor, and phosphorylation of AMPK at Thr117 can bind and activate PGC1α to initiate mitochondrial biogenesis.[45] PGC1α is expressed in many regions of the rodent brain, including the cortex, globus pallidus, hippocampus, and substantia nigra.[46] It was found that inhibition of PGC-1α expression in mice can aggravate the neurotoxicity of 1-methyl-4-phenyl-1,2,3, 6-tetrahydropyridine (MPTP) and oxidative stress factors on substantia nigra and hippocampus.[47] In contrast, over-expression of PGC1α can significantly increase mitochondrial ATP levels, maintain the stability of mitochondrial membrane potential, and protect nerve cells from oxidative stress-mediated death.[48] Our finding showed that, in HI models, AMPK/PGC1α pathway was activated but did not prevent oxidative stress and apoptosis of nerve cells. The AMPK inhibitor, CC, was

used to further investigate the possible mechanism. The protective effect of Pro was reversed by CC treatment. Therefore, we speculated that Pro might reduce apoptosis and oxidative stress by activating the AMPK/PGC1α pathway.

Mitochondria are necessary for energy production in the central nervous system (CNS) and participate in cell differentiation, apoptosis, and ROS generation.[49] TFAM is responsible for the initiation of mitochondrial DNA (mtDNA) transcription and is essential for mitochondrial biogenesis.[50] As an effector of nucleo-mitochondrial interactions, NRF1 is also known to be closely related to mitochondrial biogenesis.[51] In addition, other drugs targeting mitochondrial function have been found, such as menadione 4 and curcumin.[52,53] In neuronal cells, PGC1α has been shown to be involved in the maintenance of mtDNA transcription and replication through transcriptional regulation of NRF1 and TFAM.[54,55] However, it is not clear whether the neuroprotective effects of Pro on HIE are related to mitochondrial biogenesis. The results of this study showed that PGC1α expression was increased in the HI model, and that TFAM and NRF1 were also increased when PGC1α was upregulated by Pro. In contrast, the AMPK inhibitor CC blocked the effects of Pro on these transcription factors, suggesting that the effects of Pro on mitochondrial biogenesis may depend on PGC1α.

This work provides a new therapeutic option for HI brain injury in neonates. However, the safety of Pro and the long-term efficacy of Pro in improving learning, memory, movement and other behavioral aspects still need to be further explored. Furthermore, the combined effects of Pro with hypothermia or other neuro-protective drugs offer avenues for further research. In the absence of appropriate HIE treatment alternatives, Pro may be a viable choice for alleviate HIE's negative effects.

Although this study validated Pro to mediate neuroprotection through activation of the AMPK/PGC1α pathway in mitochondria-related mechanisms in the HI model, there were still some limitations. First, although we are confident that Pro can alleviate acute injury in HI brain damage, further studies on AMPK inhibition in vivo are needed. Although we discovered that Pro had a therapeutic impact during the acute phase of HIE and for up to 7 days following HIE, we did not investigate its long-term therapeutic and protective benefits after HIE. Second, oxygen-glucose deprivation experiments using primary neurons can better simulate the HI conditions. Finally, although we demonstrated that Pro could influence AMPK/PGC1α to regulate oxidative stress and apoptosis, other molecular pathways such as NF-κB for anti-inflammatory effects remain to be further explored.

Conclusion

In summary, the administration of Pro played a neuroprotective role in HI brain damage in rats, significantly reducing infarct volume and improving neurological prognosis. Furthermore, Pro could further activate the AMPK/PGC1α pathway to regulate the NRF1/TFAM transcription factor, thereby inhibiting neuronal oxidative stress and apoptosis. Taken together, our results suggest that Pro might serve as a potential neuroprotective agent against HI brain injury. However, long-term study is needed to determine the safety of Pro, possible side effects, and the durability of treatment. In addition, whether Pro has a therapeutic effect on other nervous system diseases characterized by mitochondrial dysfunction and oxidative stress, including stroke, mitochondrial encephalomyopathy, Parkinson's disease, etc., remains to be explored.

Data Sharing Statement

The authors will provide the raw data without undue reservation to substantiate the conclusions of this article.

Ethics Statement

The animal study was reviewed and approved by the Ethics Committee of Laboratory Animals of the Wenzhou Medical University (wydw2024-0166).

Consent for Publication

All authors approved the final manuscript and the submission to this journal.

Funding

This work was supported by the National Nature Science Foundation of China (No. 82271747), the Natural Science Foundation of Zhejiang Province (No. LY23H040004, No. LQ20H040002, No. LQ21H040009) and the Fourth Batch of Wenzhou Medical University "Outstanding and Excellent Youth Training Project" (No. 604090352/640).

Disclosure

The authors declare that they have no known competing interests for this work.

References

1. Dumbuya JS, Chen L, Wu JY, Wang B. The role of G-CSF neuroprotective effects in neonatal hypoxic-ischemic encephalopathy (HIE): current status. *J Neuroinflammation*. 2021;18(1):55. doi:10.1186/s12974-021-02084-4
2. Wood T, Osredkar D, Puchades M, et al. Treatment temperature and insult severity influence the neuroprotective effects of therapeutic hypothermia. *Sci Rep*. 2016;6(1):23430. doi:10.1038/srep23430
3. Wassink G, Davidson JO, Dhillon SK, et al. Therapeutic hypothermia in neonatal hypoxic-ischemic encephalopathy. *Curr Neurol Neurosci Rep*. 2019;19(2):2. doi:10.1007/s11910-019-0916-0
4. Yang M, Wang K, Liu B, Shen Y, Liu G. Hypoxic-ischemic encephalopathy: pathogenesis and promising therapies. *Molecular Neurobiol*. 2024:1–8.
5. Serrenho I, Rosado M, Dinis A, et al. Stem cell therapy for neonatal hypoxic-ischemic encephalopathy: a systematic review of preclinical studies. *Int J Mol Sci*. 2021;22(6):3142. doi:10.3390/ijms22063142
6. Zhao M, Zhu P, Fujino M, et al. Oxidative stress in hypoxic-ischemic encephalopathy: molecular mechanisms and therapeutic strategies. *Int J Mol Sci*. 2016;17(12):2078. doi:10.3390/ijms17122078
7. Yuan Y, Tian Y, Jiang H, et al. Mechanism of PGC-1α-mediated mitochondrial biogenesis in cerebral ischemia-reperfusion injury. *Front Mol Neurosci*. 2023;16:1224964. doi:10.3389/fnmol.2023.1224964
8. Chen SD, Yang DI, Lin TK, Shaw FZ, Liou CW, Chuang YC. Roles of oxidative stress, apoptosis, PGC-1α and mitochondrial biogenesis in cerebral ischemia. *Int J Mol Sci*. 2011;12(10):7199–7215. doi:10.3390/ijms12107199
9. Huang J, Liu W, Doycheva DM, et al. Ghrelin attenuates oxidative stress and neuronal apoptosis via GHSR-1α/AMPK/Sirt1/PGC-1α/UCP2 pathway in a rat model of neonatal HIE. *Free Radic Biol Med*. 2019;141:322–337. doi:10.1016/j.freeradbiomed.2019.07.001
10. Xiong LL, Xue LL, Du RL, et al. Vi4-miR-185-5p-Igfbp3 network protects the brain from neonatal hypoxic ischemic injury via promoting neuron survival and suppressing the cell apoptosis. *Front Cell Develop Biol*. 2020;8:529544. doi:10.3389/fcell.2020.529544
11. Gendi F, Pei F, Wang Y, Li H, Fu J, Chang C. Mitochondrial proteins unveil the mechanism by which physical exercise ameliorates memory, learning and motor activity in hypoxic ischemic encephalopathy rat model. *Int J Mol Sci*. 2022;23(8):4235. doi:10.3390/ijms23084235
12. Yin W, Signore AP, Iwai M, Cao G, Gao Y, Chen J. Rapidly increased neuronal mitochondrial biogenesis after hypoxic-ischemic brain injury. *Stroke*. 2008;39(11):3057–3063. doi:10.1161/STROKEAHA.108.520114
13. Barone E, Di Domenico F, Perluigi M, Butterfield DA. The interplay among oxidative stress, brain insulin resistance and AMPK dysfunction contribute to neurodegeneration in type 2 diabetes and Alzheimer disease. *Free Radic Biol Med*. 2021;176:16–33.
14. Rodríguez C, Muñoz M, Contreras C, Prieto D. AMPK, metabolism, and vascular function. *FEBS J*. 2021;288(12):3746–3771. doi:10.1111/febs.15863
15. Wang Y, Guan X, Gao CL, et al. Medioresinol as a novel PGC-1α activator prevents pyroptosis of endothelial cells in ischemic stroke through PPARα-GOT1 axis. *Pharmacol Res*. 2021;169:105640. doi:10.1016/j.phrs.2021.105640
16. Houten SM, Auwerx J. PGC-1alpha: turbocharging mitochondria. *Cell*. 2004;119(1):5–7. doi:10.1016/j.cell.2004.09.016
17. Hao L, Zhong W, Dong H, et al. ATF4 activation promotes hepatic mitochondrial dysfunction by repressing NRF1-TFAM signalling in alcoholic steatohepatitis. *Gut*. 2021;70(10):1933–1945. doi:10.1136/gutjnl-2020-321548
18. Zhao M, Wang Y, Li L, et al. Mitochondrial ROS promote mitochondrial dysfunction and inflammation in ischemic acute kidney injury by disrupting TFAM-mediated mtDNA maintenance. *Theranostics*. 2021;11(4):1845–1863. doi:10.7150/thno.50905
19. Alam MB, Ju MK, Kwon YG, Lee SH. Protopine attenuates inflammation stimulated by carrageenan and LPS via the MAPK/NF-κB pathway. *Food Chem Toxicol*. 2019;131:110583. doi:10.1016/j.fct.2019.110583
20. Bae DS, Kim YH, Pan CH, et al. Protopine reduces the inflammatory activity of lipopolysaccharide-stimulated murine macrophages. *BMB Reports*. 2012;45(2):108–113. doi:10.5483/BMBRep.2012.45.2.108
21. Son Y, An Y, Jung J, et al. Protopine isolated from Nandina domestica induces apoptosis and autophagy in colon cancer cells by stabilizing p53. *Phytotherapy Res*. 2019;33(6):1689–1696. doi:10.1002/ptr.6357
22. Xiao X, Liu J, Hu J, et al. Protective effects of protopine on hydrogen peroxide-induced oxidative injury of PC12 cells via Ca(2+) antagonism and antioxidant mechanisms. *Eur J Pharmacol*. 2008;591(1–3):21–27. doi:10.1016/j.ejphar.2008.06.045
23. Rathi A, Srivastava AK, Shirwaikar A, Singh Rawat AK, Mehrotra S. Hepatoprotective potential of Fumaria indica Pugsley whole plant extracts, fractions and an isolated alkaloid protopine. *Phytomedicine*. 2008;15(6–7):470–477. doi:10.1016/j.phymed.2007.11.010
24. Nie C, Wang B, Wang B, Lv N, Yu R, Zhang E. Protopine triggers apoptosis via the intrinsic pathway and regulation of ROS/PI3K/Akt signalling pathway in liver carcinoma. *Can Cell Inter*. 2021;21(1):396. doi:10.1186/s12935-021-02105-5
25. Orhana I, Ozçelik B, Karaoğlu T, Sener B. Antiviral and antimicrobial profiles of selected isoquinoline alkaloids from Fumaria and Corydalis species. *Z Naturforsch C*. 2007;62(1–2):19–26. doi:10.1515/znc-2007-1-204
26. Sreenivasmurthy SG, Iyaswamy A, Krishnamoorthi S, et al. Protopine promotes the proteasomal degradation of pathological tau in Alzheimer's disease models via HDAC6 inhibition. *Phytomedicine*. 2022;96:153887. doi:10.1016/j.phymed.2021.153887
27. Xu LF, Chu WJ, Qing XY, et al. Protopine inhibits serotonin transporter and noradrenaline transporter and has the antidepressant-like effect in mice models. *Neuropharmacology*. 2006;50(8):934–940. doi:10.1016/j.neuropharm.2006.01.003
28. Xiao X, Liu J, Hu J, Li T, Zhang Y. Protective effect of protopine on the focal cerebral ischaemic injury in rats. *Basic Clin Physiol Pharmacol*. 2007;101(2):85–89. doi:10.1111/j.1742-7843.2007.00075.x
29. Bournine L, Bensalem S, Wauters JN, et al. Identification and quantification of the main active anticancer alkaloids from the root of Glaucium flavum. *Int J Mol Sci*. 2013;14(12):23533–23544. doi:10.3390/ijms141223533
30. Xu Y, Sun J, Li W, et al. Analgesic effect of the main components of Corydalis yanhusuo (yanhusuo in Chinese) is caused by inhibition of voltage gated sodium channels. *J Ethnopharmacol*. 2021;280:114457. doi:10.1016/j.jep.2021.114457

31. Wang G, Hazra TK, Mitra S, Lee HM, Englander EW. Mitochondrial DNA damage and a hypoxic response are induced by CoCl(2) in rat neuronal PC12 cells. *Nucleic Acids Res*. 2000;28(10):2135–2140. doi:10.1093/nar/28.10.2135
32. Vannucci RC, Vannucci SJ. Perinatal hypoxic-ischemic brain damage: evolution of an animal model. *Dev Neurosci*. 2005;27(2–4):81–86. doi:10.1159/000085978
33. Blokhina O, Virolainen E, Fagerstedt KV. Antioxidants, oxidative damage and oxygen deprivation stress: a review. *Ann Bot*. 2003;91(2):179–194. doi:10.1093/aob/mcf118
34. He Y, Gan X, Zhang L, et al. CoCl(2) induces apoptosis via a ROS-dependent pathway and Drp1-mediated mitochondria fission in periodontal ligament stem cells. *Am J Physiol Cell Physiol*. 2018;315(3):C389–c397. doi:10.1152/ajpcell.00248.2017
35. DeGiosio RA, Grubisha MJ, MacDonald ML, McKinney BC, Camacho CJ, Sweet RA. More than a marker: potential pathogenic functions of MAP2. *Front Mol Neurosci*. 2022;15:974890. doi:10.3389/fnmol.2022.974890
36. Pettigrew LC, Holtz ML, Craddock SD, Minger SL, Hall N, Geddes JW. Microtubular proteolysis in focal cerebral ischemia. *J Cerebral Blood Flow Metabolism*. 1996;16(6):1189–1202. doi:10.1097/00004647-199611000-00013
37. Liu B, Xin W, Tan JR, et al. Myelin sheath structure and regeneration in peripheral nerve injury repair. *Proc Natl Acad Sci*. 2019;116 (44):22347–22352. doi:10.1073/pnas.1910292116
38. Keam SJ. Sovateltide: first Approval. *Drugs*. 2023;83(13):1239–1244. doi:10.1007/s40265-023-01922-4
39. Nair J, Kumar VHS. Current and emerging therapies in the management of hypoxic ischemic encephalopathy in neonates. *Children*. 2018;5(7). doi:10.3390/children5070099
40. Hassan W, Noreen H, Rehman S, Kamal MA, da Rocha JBT. Association of oxidative stress with neurological disorders. *Curr Neuropharmacol*. 2022;20(6):1046–1072. doi:10.2174/1570159X19666211111141246
41. Qin X, Cheng J, Zhong Y, et al. Mechanism and treatment related to oxidative stress in neonatal hypoxic-ischemic encephalopathy. *Front Mol Neurosci*. 2019;12:88. doi:10.3389/fnmol.2019.00088
42. Pizzino G, Irrera N, Cucinotta M, et al. Oxidative stress: harms and benefits for human health. *Oxid Med Cell Longev*. 2017;2017:8416763. doi:10.1155/2017/8416763
43. Chen Z, Wang C, Yu N, et al. INF2 regulates oxidative stress-induced apoptosis in epidermal HaCaT cells by modulating the HIF1 signaling pathway. *Biomed Pharmacothe*. 2019;111:151–161. doi:10.1016/j.biopha.2018.12.046
44. Jiang S, Li T, Ji T, et al. AMPK: potential therapeutic target for ischemic stroke. *Theranostics*. 2018;8(16):4535–4551. doi:10.7150/thno.25674
45. Rius-Pérez S, Torres-Cuevas I, Millán I, Ortega ÁL, Pérez S. PGC-1α, inflammation, and oxidative stress: an integrative view in metabolism. *Oxid Med Cell Longev*. 2020;2020:1452696. doi:10.1155/2020/1452696
46. Tritos NA, Mastaitis JW, Kokkotou EG, Puigserver P, Spiegelman BM, Maratos-Flier E. Characterization of the peroxisome proliferator activated receptor coactivator 1 alpha (PGC 1alpha) expression in the murine brain. *Brain Res*. 2003;961(2):255–260. doi:10.1016/S0006-8993(02)03961-6
47. St-Pierre J, Drori S, Uldry M, et al. Suppression of reactive oxygen species and neurodegeneration by the PGC-1 transcriptional coactivators. *Cell*. 2006;127(2):397–408. doi:10.1016/j.cell.2006.09.024
48. Ye Q, Huang W, Li D, et al. Overexpression of PGC-1α influences mitochondrial signal transduction of dopaminergic neurons. *Molecular Neurobiol*. 2016;53(6):3756–3770. doi:10.1007/s12035-015-9299-7
49. Xu W, Yan J, Ocak U, et al. Melanocortin 1 receptor attenuates early brain injury following subarachnoid hemorrhage by controlling mitochondrial metabolism via AMPK/SIRT1/PGC-1α pathway in rats. *Theranostics*. 2021;11(2):522–539. doi:10.7150/thno.49426
50. Santos JM, Tewari S, Goldberg AF, Kowluru RA. Mitochondrial biogenesis and the development of diabetic retinopathy. *Free Radic Biol Med*. 2011;51(10):1849–1860. doi:10.1016/j.freeradbiomed.2011.08.017
51. Zhao T, Zhang J, Lei H, et al. NRF1-mediated mitochondrial biogenesis antagonizes innate antiviral immunity. *EMBO J*. 2023;42(16):e113258. doi:10.15252/embj.2022113258
52. Feng X, Zheng Y, Mao N, et al. Menaquinone-4 alleviates hypoxic-ischemic brain damage in neonatal rats by reducing mitochondrial dysfunction via Sirt1-PGC-1α-TFAM signaling pathway. *Int Immunopharmacol*. 2024;134:112257. doi:10.1016/j.intimp.2024.112257
53. Rocha-Ferreira E, Sisa C, Bright S, et al. Curcumin: novel treatment in neonatal hypoxic-ischemic brain injury. *Front Physiol*. 2019;10:1351. doi:10.3389/fphys.2019.01351
54. Fan H, Ding R, Liu W, et al. Heat shock protein 22 modulates NRF1/TFAM-dependent mitochondrial biogenesis and DRP1-sparked mitochondrial apoptosis through AMPK-PGC1α signaling pathway to alleviate the early brain injury of subarachnoid hemorrhage in rats. *Redox Biol*. 2021;40:101856. doi:10.1016/j.redox.2021.101856
55. Li L, Xiao L, Hou Y, et al. Sestrin2 silencing exacerbates cerebral ischemia/reperfusion injury by decreasing mitochondrial biogenesis through the AMPK/PGC-1α pathway in rats. *Sci Rep*. 2016;6(1):30272. doi:10.1038/srep30272